Studying Typhoon Morakot with a Coupled WRFDA-DART System

Craig Schwartz[1*1], Zhiquan Liu[1], Yongsheng Chen[2], Xiang-Yu Huang[1]

[1]*NCAR Earth System Laboratory/Mesoscale and Microscale Meteorology Division*
[2]*York University*

1. Introduction

The direct assimilation of satellite radiance observations is an important component of global numerical weather prediction (NWP) data assimilation (DA) systems at many operational meteorological centers (e.g., Caplan et al. 1997; Zapotocny et al. 2007; Gauthier et al. 2007; Rawlins et al. 2007; Karbou et al. 2010). As the information from radiances leads to specification of initial conditions (ICs) that are closer to the true atmospheric state, radiance DA has been shown to substantially improve weather forecasts, especially over maritime areas and the southern hemisphere, where there are fewer conventional observations (Caplan et al. 1997; Derber and Wu 1998; Zapotocny et al. 2005, 2007).

However, analysis and forecast sensitivity to radiance DA within *regional* NWP models has been less-rigorously examined, and the few studies assessing this sensitivity have yielded somewhat ambiguous results. For instance, Xu et al. (2009a) assimilated radiances over southwest Asia with the Gridpoint Statistical Interpolation (GSI; Kleist et al. 2009) analysis system and found that forecasts were improved in some sub-regions but degraded in others. Additionally, Xu et al. (2009b) noted that radiances from some satellite sensors generated a "limited improvement" regarding track forecasts of hurricane Katrina while radiances from other sensors had little impact. They also found that radiance DA did not alter intensity forecasts of Katrina. Similarly, an earlier DA study over North America revealed that certain satellite sensors impacted weather forecasts, while others had little effect (Zapotocny et al. 2005).

Clearly, there remain questions regarding the benefit of assimilating radiances within regional DA/NWP systems. Yet, as the use of regional NWP has proliferated in the past decade thanks to community models such as the Weather Research and Forecast (WRF; Skamarock et al. 2008) model, it is important to understand how radiance DA can improve limited-area forecasts, especially for domains spanning data-sparse areas (such as deserts or oceans). Moreover, while ensemble DA techniques such as the ensemble Kalman filter (EnKF; Evensen 2003) have been shown to be appropriate for regional models (e.g., Meng and Zhang 2008), to our knowledge, there have been no attempts to directly assimilate satellite radiances over a limited-area domain using ensemble DA methods.

Thus, in recognition of the uncertainty associated with assimilating radiances in a regional model, this work investigates radiance DA in both deterministic and ensemble

**Corresponding author email address: schwartz@ucar.edu*

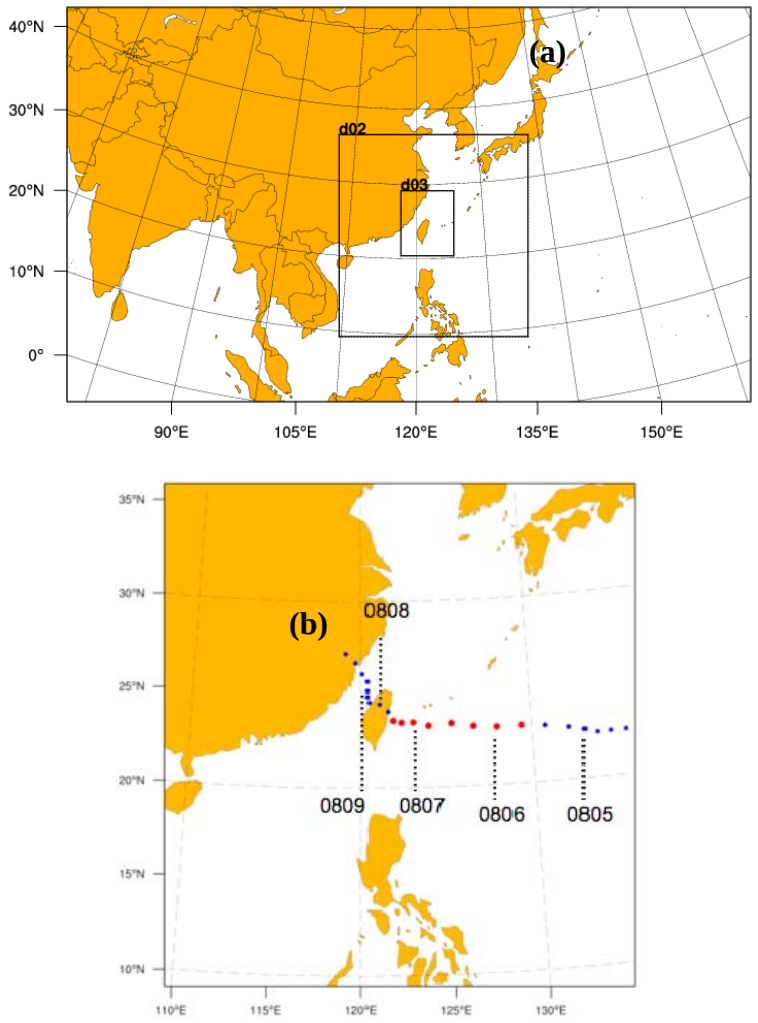

Fig. 1. (a) Computational domain used for all experiments and (b) track of typhoon Morakot overlaid on d02. In (b), the estimated center of circulation of Morakot is plotted every 6-hrs. Red (blue) dots indicate Morakot was at typhoon (tropical storm or depression) strength, and numbers refer to the month and day at 0000 UTC in 2009 (e.g., 0809 means 0000 UTC 09 August 2009).

frameworks while studying typhoon Morakot, which formed in the western Pacific Ocean in August 2009 and made landfalls in both Taiwan and China (Fig. 1b). All weather forecasts were generated by the Advanced Research Weather Research and Forecast model (WRF-ARW; Skamarock et al. 2008), while the DA techniques differed. Deterministic experiments used the WRF data assimilation (WRFDA; Skamarock et al. 2008) package to produce analyses using a 3-dimensional variational (3DVAR; Barker et al. 2003,2004) technique. On the other hand, the ensemble experiments used software from the Data Assimilation Research Testbed (DART; Anderson et al. 2009) to generate analyses with a 64-member ensemble using the Ensemble Adjustment Filter (EAF; Anderson 2001; Liu et al. 2007). In order to take advantage of observation processing and quality control (QC) in WRFDA, we used WRFDA in the ensemble DA process and describe the practical implementation and benefits of this unique coupling.

While several studies have directly compared variational and ensemble DA techniques (e.g., Houtekamer et al. 2005; Meng and Zhang 2008; Whitaker et al. 2008; Buehner et al. 2010a,b), here we limit direct comparison between the ensemble and deterministic experiments and focus instead on the impact of radiance DA within the two datasets. Section 2 details model configurations and the experimental setup, while section 3 describes the implementation and rationale for the WRFDA-DART coupled system. Results are presented in section 4 before concluding in section 5.

2. Model configurations and experimental design

While deterministic and ensemble NWP systems inherently differ, a number of settings were fixed for all experiments. These general parameters are now described before detailing the individual experimental configurations.

a. Common configuration settings

All experiments ran over the same triple-nested computational domain (Fig. 1a) and a new 72-hr weather forecast was generated by version 3.1.1 of the WRF-ARW model every 6 hours beginning 1800 UTC 03 August 2009 and ending 1200 UTC 09 August 2009, inclusive (hereafter, "experimental period"). Horizontal grid spacing in the outermost domain (d01) was 45-km and the grid length was reduced by a factor of three in each nest. That is, the innermost domain (d03) used 5-km horizontal grid spacing and the grid length in the middle domain (d02) was 15-km. There were forty-five (45) vertical levels and the model top was 30-hPa. Physical parameterizations were held constant across the three domains and experiments, except no cumulus parameterization scheme was used in d03. Lateral boundary conditions (LBCs) for the WRF forecasts were provided by the Global Forecast System (GFS).

Many aspects regarding DA were also common to all experiments. An observation window of ± 3 hours from the analysis time was used for all observation types, and DA was performed in the outer domain (d01) only. Additionally, each experiment employed "full-cycling" with a six-hourly period. More specifically, the previous 6-hr forecast served as the background (or "first-guess") for the current analysis cycle and subsequent WRF forecasts. None of the experiments used any type of cyclone relocation. Thus, analyses and forecasts were prone to large track errors if previous forecasts were erroneous.

The specific deterministic and ensemble settings are now described.

b. Deterministic configurations

DA in the deterministic configurations was performed using WRFDA's 3DVAR technique using a regional background error (BE) covariance matrix generated specifically for this domain (Fig. 1a) using the "NMC method" (Parrish and Derber

1992). This formulation of the BE is flow-independent and differs significantly from the specification of the BE in the ensemble system.

WRFDA's 3DVAR system generates a best-fit "analysis" considering two sources of initial information: 1) observations at irregularly spaced points, and 2) a background (or "first-guess") field, typically taken to be a short-term, gridded model forecast. Associated with the background and observations are their error characteristics. Given the background, observations, and errors, the analysis (**x**) can be determined by minimizing a scalar cost-function (*J*) given by

$$J(\mathbf{x}) = \frac{1}{2}(\mathbf{x} - \mathbf{x_B})^{\mathrm{T}} \mathbf{B}^{-1} (\mathbf{x} - \mathbf{x_B}) + \frac{1}{2}[\mathbf{y} - H(\mathbf{x})]^{\mathrm{T}} \mathbf{R}^{-1} [\mathbf{y} - H(\mathbf{x})], \qquad (1)$$

where, $\mathbf{x_B}$ denotes the background, **y** is the observations, and **B** and **R** represent the background and observation error covariances, respectively. *H* is the (potentially non-linear) "observation operator" that transforms model-predicted variables to observed quantities and interpolates values at grid-points to the observation locations. To assimilate satellite radiances, a radiative transfer model (RTM) is coupled to the 3DVAR system and used as an observation operator to convert the temperature and humidity profiles into brightness temperatures. Eq. (1) is solved iteratively until the value of **x** is found that minimizes *J*, and can be rewritten as

$$J = J_B + J_O, \qquad (2)$$

where J_B and J_O are the first and second terms on the RHS of Eq. (1) that represent the relative contribution to *J* from the background and observations, respectively.

The GFS analysis valid 1200 UTC 03 August served as the initial conditions (ICs) to generate a 6-hr WRF forecast (valid 1800 UTC 03 August) that was used as the background for the first analysis. Two deterministic cycling experiments ran throughout the experimental period and were configured similarly, except the first experiment (3dvar_conv) assimilated solely conventional observations[2], including metar, synop, ship, buoy, and radiosonde data, while the second (3dvar_conv+RAD) also assimilated satellite radiances. Each analysis (every 6-hrs) initialized a 72-hr WRF-ARW forecast. Given these configurations, the impact of satellite radiance DA was clearly isolated and assessed.

The experiment that assimilated radiances used data from Advanced Microwave Sounding Units A and B (AMSU-A, AMSU-B) and Microwave Humidity Sounder (MHS) sensors outfitted on NOAA's Polar Orbiting Environmental Satellites (POES). The AMSU-A sensor is most sensitive to the atmosphere's temperature profile, while the AMSU-B and MHS sensors are most sensitive to moisture. All satellite data were thinned on a 90-km mesh grid and subjected to variational bias correction (Auligné et al. 2007). Radiances were assimilated over land and sea, but QC settings only permitted non-precipitating sky radiances to be assimilated. Table 1 lists the satellite IDs, sensors,

[2]Herein, "conventional observations" means all observations that are *not* radiances.

and channels that were used. As satellite positions change with time, data from a given satellite may have been unavailable over the computational domain at a particular analysis time.

Satellite ID	Sensor	Channels
NOAA-15	AMSU-A	4,5,6,7,8
NOAA-15	AMSU-B	3,5
NOAA-18	AMSU-A	4,5,6,7,8
NOAA-18	MHS	3,4,5
METOP-02	AMSU-A	4,5,6,8
METOP-02	MHS	3,4,5

Table 1. Satellite IDs, sensors, and channels used in the experiments that assimilated radiances.

c. Ensemble configurations

A 64-member ensemble was initially constructed by randomly perturbing the 1200 UTC 03 August GFS analysis. Using these perturbed ICs, a 6-hr forecast was run for each member (valid 1800 UTC 03 August), and these backgrounds were used as input for the first DART-EAF analysis.

The EAF generates background error covariances by using flow-dependent statistics from the ensemble. For a detailed description of the EAF, the reader is referred to Anderson (2001) and Eqs. 2.1-2.13 in Liu. et al. (2007).

Two ensemble experiments were run that were configured similarly to the deterministic tests. The first (DART_conv) utilized the full suite of conventional observations, while the second (DART_conv+RAD) assimilated radiances, as well (Table 1), thus permitting an assessment of the impact of satellite DA within an ensemble framework. A mean analysis was computed each DA cycle (every 6-hrs) and used as the ICs for 72-hr WRF-ARW forecasts.

The four experiments are summarized in Table 2. Given the similar experimental designs within the deterministic and ensemble sets, it is interesting to compare the two sets. While we will mention interesting differences between the ensemble and deterministic output, we stress that a rigorous comparison of the merits of ensemble versus deterministic DA and modeling is not the intent of this paper.

Experiment Name	Type	Radiances Assimilated?
3dvar_conv	Deterministic	No
3dvar_conv+RAD	Deterministic	Yes
DART_conv	Ensemble	No
DART_conv+RAD	Ensemble	Yes

Table 2. Summary of the four experiments.

3. Coupling of WRFDA and DART

The ensemble experiments used DART to generate each EAF analysis. However, DART can only process input observations if they are in the DART-specific "observation sequence" format (explained at http://www.image.ucar.edu/DAReS/DART/DART_Observations.php). While some codes to convert various observation formats into the observation sequence are provided in the DART package, it is ultimately the user's responsibility to properly encode the observations.

We used WRFDA-3DVAR as an intermediate step in the production of the observation sequence. Currently, WRFDA can process input conventional observations in both "little_r" ascii and NCEP PREPBUFR formats. Radiances are solely processed in BUFR format. Although little_r and PREPBUFR data can be converted directly into the DART format, there are several advantages to using WRFDA as an intermediate step to produce the observation sequence. For example, WRFDA's QC features are used to reject observations deemed likely to be incorrect based on the first-guess field, thus preventing bad data from entering DART. Additionally, observational error characteristics are assigned through WRFDA and subsequently used in DART.

However, the greatest benefits from this procedure are realized when satellite radiances are assimilated. In fact, currently, satellite radiance measurements cannot be imported directly into DART since DART is not coupled to a RTM. But, as WRFDA *is* coupled to a RTM, it can easily calculate the brightness temperatures from the temperature and humidity profiles. Additionally, the raw brightness temperatures require bias correction, which cannot be done by DART but is accomplished quickly and easily by WRFDA. WRFDA also QCs the brightness temperatures.

Practical implementation of the WRFDA/DART coupling is now detailed.

a) Conventional observations

Consider an ensemble comprised of $k = 1,2, \ldots, n$ members and p_c conventional observations at a given analysis time (for our ensemble, $n = 64$). Therefore, there were n background fields (from the previous cycle's short-term forecasts). First, WRFDA-3DVAR was run a total of n times without iterative minimization (zero iterations) using the same input observations but the kth member's background field as input. Even without iterative minimization, WRFDA's observation operators were applied to the kth background at each of the p_c points. Output from each 3DVAR run contained the observation values (identical for each of the n runs), innovations (observation minus background), QC information, and observation error characteristics at each of the p_c locations. Given the innovation and observation, the background value at the p_cth observation point was obtained for the kth member.

Next, a maximum of $n*p_c$ point background values and p_c observations were converted into the DART observation sequence format. Given the n background fields, it was

possible that some members rejected a particular observation (based on the innovation and observational error characteristics) while other members accepted it. A conventional observation was only inserted into the observation sequence if it passed the QC standards for *all* members. Finally, while DART typically applies forward observation operators to the prior (state before assimilation) ensemble, since the observation operators were applied using 3DVAR and the background values at observations points were placed in the observation sequence, the DART code was modified to skip the application of these prior operators. DART observation operators were only applied to the posterior (state immediately after assimilation) ensemble.

b) Satellite radiances/brightness temperatures

The process to code brightness temperatures in the observation sequence followed the same procedure as the conventional observations, but there were a few additional complexities. First, whereas each conventional observation was associated with a specific vertical level, radiances were not. Rather, information throughout the atmospheric column was used to determine the brightness temperature. However, we provided DART with an approximate vertical location for each brightness temperature by utilizing the weighting function (Petty 2004) at each grid-point where a radiance was assimilated. The weighting function provides information about the vertical level(s) that contribute most to the change in brightness temperature. Specifically, the vertical level for each brightness temperature was specified as the model level at which the weighting function was maximized.

Second, for radiance processing, we only utilized QC flags and observation errors from the 3DVAR run that used the mean background field as input. This method differs from the manner in which conventional observations were treated, where only those conventional observations that passed QC tests for each ensemble member were kept. However, had we followed the approach used for conventional observations, about 50% fewer brightness temperatures would have been assimilated in the ensemble experiment.

Fig. 2 reveals this method permitted the assimilation of comparable numbers of radiance observations in both the DART_conv+RAD and 3dvar_conv+RAD experiments. In fact, slightly more radiances were assimilated by the DART_conv+RAD experiment than the 3dvar_conv+RAD experiment, likely because the ensemble mean background field was better than the deterministic first-guess, thus leading to fewer rejected observations.

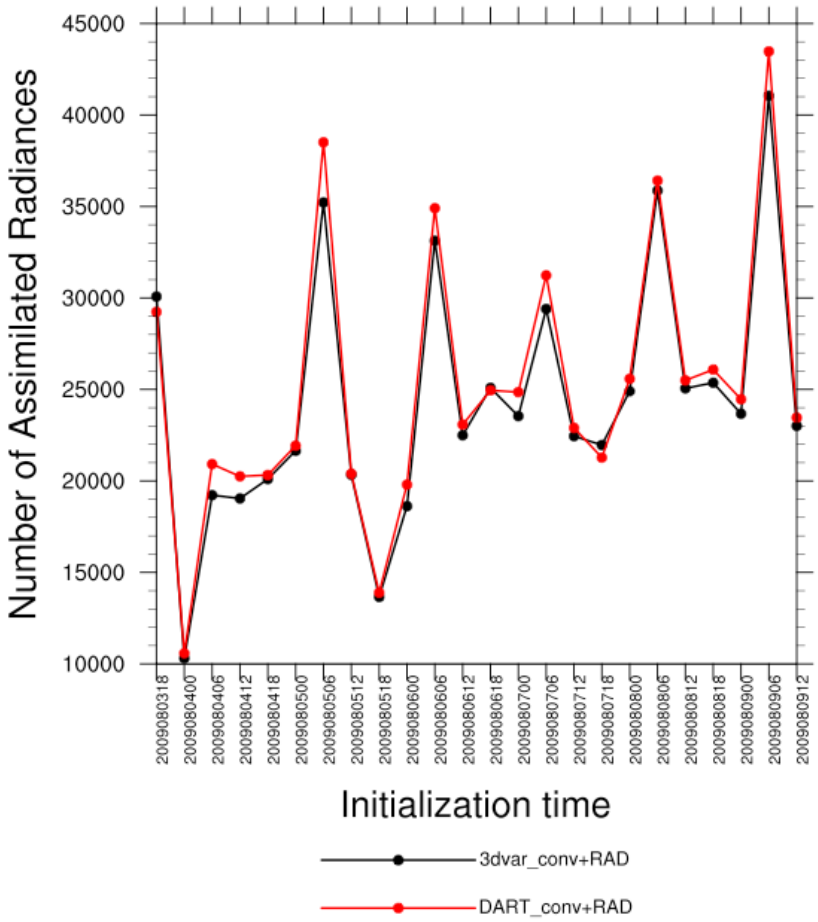

Fig. 2. Total number of brightness temperature observations that were actually assimilated for each analysis. See Table 2 for meaning of the legend.

4. Results

The "best-track" analysis of typhoon Morakot by the Joint Typhoon Warning Center (JTWC) was used as "truth" when verifying model forecasts and analyses of maximum wind speed (WS_{max}), minimum sea-level pressure (SLP_{min}), and track. Verification was performed on the native model grids, and we focus on results from the middle domain (d02), aggregated over all forecasts and analyses from 1800 UTC 04 August through 1200 UTC 09 August, inclusive.

a) Track errors

While the 3dvar_conv+RAD experiment produced better average analyses and 6-hr forecasts of Morakot's track (Fig. 3) than the 3dvar_conv experiment, after the 12-hr forecast time, the two curves intersected several times, indicating neither experiment improved over the other at forecast lengths > 12-hrs. The two ensemble experiments generated similar mean track errors, as well. It is noteworthy that after the 36-hr time

period track forecasts from the ensemble were substantially better than those from the deterministic experiments.

b) Minimum SLP errors

The large (10-19 hPa) SLP_{min} errors (Fig. 4) can be attributed to the relatively coarse horizontal grid spacing (15-km) in the middle domain. Nonetheless, there were distinct trends amongst the experiments. For example, with the exception of the 72-hr forecast time, the 3dvar_conv+RAD experiment yielded better SLP_{min} forecasts than the 3dvar_conv experiment. Similarly, assimilating radiances within the ensemble forecasting system resulted in SLP_{min} errors that were lower than those when radiances were not assimilated.

c) Maximum wind speed errors

WS_{max} error trends (Fig. 5) were similar to those of SLP_{min}. The ensemble DART_conv+RAD experiment produced better forecasts than the DART_conv experiment. Additionally, after 18 hours, the 3DVAR experiment with radiances produced better forecasts than the experiment without radiances.

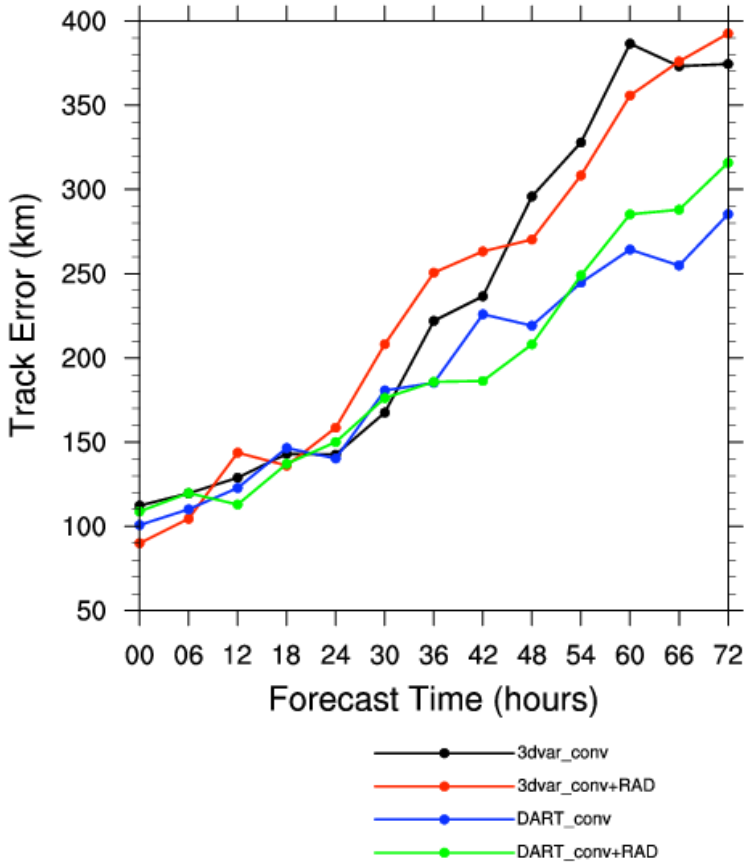

Fig. 3. Average track error (km) for selected forecast hours during the period spanning 1800 UTC 04 August through 1200 09 August, inclusive.

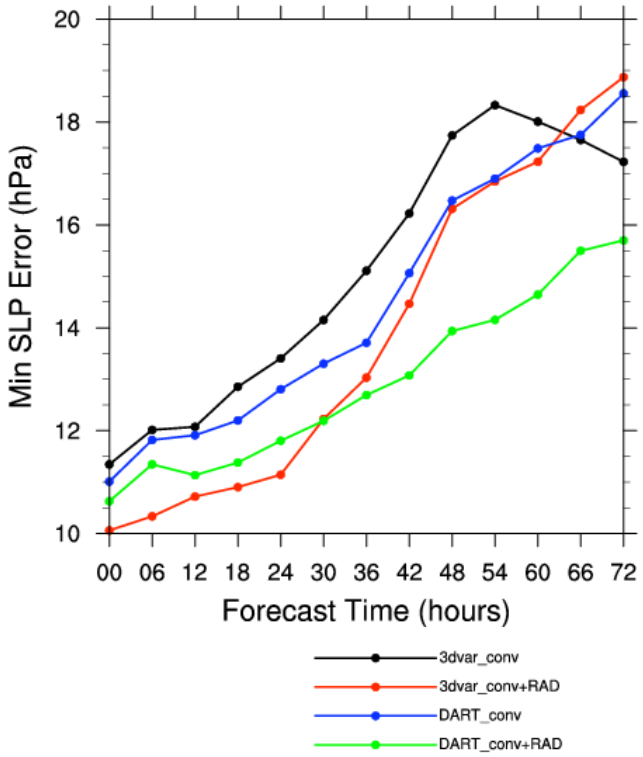

Fig. 4. As in Fig. 3, but minimum SLP error (hPa).

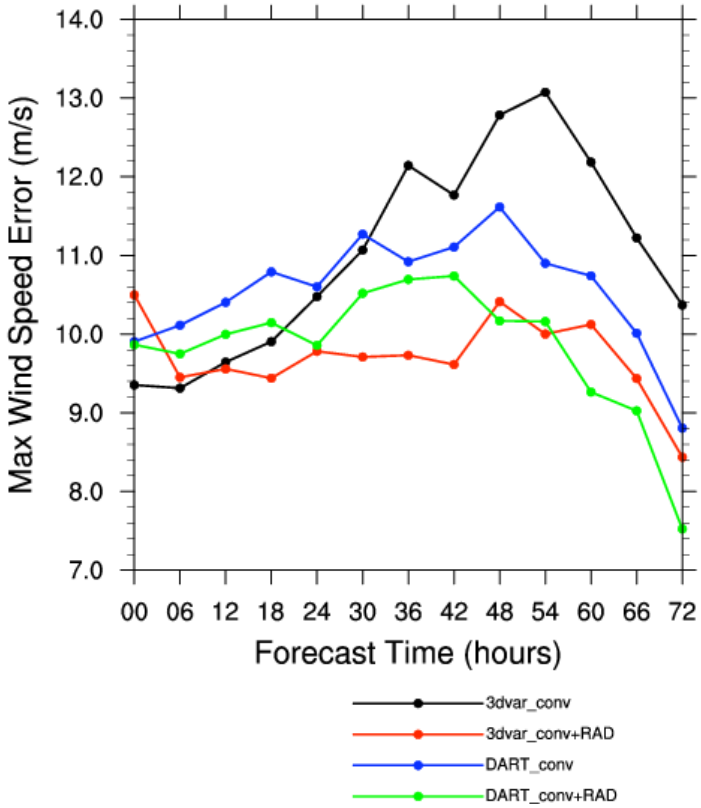

Fig. 5. As in Fig. 3, but for maximum wind speed error (m/s).

5. Discussion and summary

DA in both deterministic and ensemble frameworks was employed to study typhoon Morakot between 03 and 09 August 2009. All experiments used 6-hrly full-cycling and produced 72-hr forecasts 4 times per day (from the mean analysis in the ensemble experiments). The experiments were configured to clearly isolate the impact of assimilating AMSU satellite radiances in regional deterministic and ensemble settings.

The deterministic experiments used a 3DVAR DA system, while the ensemble experiments used a coupled WRFDA-DART system. While it is not necessary to couple DART to WRFDA if just conventional observations are desired, the coupled system allows for improved QC of the observations. However, when radiances are assimilated, coupling DART to WRFDA is critical to permit proper QC and bias correction of brightness temperatures.

On average, those experiments that assimilated radiances produced better forecasts of minimum sea level pressure and maximum wind speeds than the corresponding experiments that assimilated conventional observations only. Therefore, the addition of satellite radiances into the observational datastream may be helpful for predicting the intensity of tropical cyclones (TCs). However, track forecasts within the two datasets behaved similarly, in that assimilating radiances did not appear to have a clear impact.

The marginal impact of radiances on TC track forecasts is not without precedent, as Zapotocny et al. (2007) noted that forecasts of TC tracks were relatively insensitive to radiance data. At this time, the reasons for tfhis behavior are unclear and warrant more study, as satellite radiances can provide a wealth of data in oceanic areas where TCs roam. Additional studies assimilating satellite radiances in regional settings are encouraged.

References

Anderson, J. L., 2001: An ensemble adjustment Kalman filter for data assimilation. *Mon. Wea. Rev.*, **129**:2884–2903.

Anderson, J. L., T. Hoar, K. Raeder, H. Liu, N. Collins, R. Torn, and A. Avellano, 2009: The Data Assimilation Research Testbed: A community data assimilation facility. *Bull. Amer. Meteor. Soc.*, **90**:1283–1296.

Auligné T, A.P. McNally, and D.P. Dee, 2007. Adaptive bias correction for satellite data in a numerical weather prediction system. *Quarterly Journal of the Royal Meteorological Society* **133**: 631-642.

Barker, D. M., W. Huang, Y-R. Guo, and A. Bourgeois, 2003: A three-dimensional variational (3DVAR) data assimilation system for use with MM5. NCAR Tech. Note.

NCAR/TN-453+STR, 68 pp. [Available from UCAR Communications, P.O. Box 3000, Boulder, CO 80307.]

Barker, D. M., W. Huang, Y-R. Guo, A. Bourgeois, and X. N. Xio, 2004: A three-dimensional variational data assimilation system for MM5: Implementation and initial results. *Mon. Wea. Rev.*, **132**:897–914.

Buehner, M., P. L. Houtekamer, C. Charette, H. L. Mitchell, and B. He, 2010a: Intercomparison of Variational Data Assimilation and the Ensemble Kalman Filter for Global Deterministic NWP. Part I: Description and single-observation experiments. *Mon. Wea. Rev.* In press.

Buehner, M., P. L. Houtekamer, C. Charette, H. L. Mitchell, and B. He, 2010b: Intercomparison of Variational Data Assimilation and the Ensemble Kalman Filter for Global Deterministic NWP. Part II: One-Month Experiments with Real Observations. *Mon. Wea. Rev.* In press.

Caplan, P., J. C. Derber, W. Gemmill, S. Hong, H. Pan, and D. F. Parrish, 1997: Changes to the 1995 NCEP operational Medium-Range Forecast model analysis–forecast system. *Wea. Forecasting*, **12**:581–594.

Derber, J. C. and W-S. Wu, 1998: The use of TOVS cloud-cleared radiances in the NCEP SSI analysis system. *Mon. Wea. Rev.*, **126**:2287–2299.

Evensen, G. 2003. The ensemble Kalman filter: Theoretical formulation and practical implementation. Ocean Dyn. 53:343–367.

Gauthier, P., M. Tanguay, S. Laroche, S. Pellerin, and J. Morneau, 2007: Extension of 3DVAR to 4DVAR: Implementation of 4DVAR at the Meteorological Service of Canada. *Mon. Wea. Rev.*, **135**:2339–2354.

Houtekamer, P. L., H. L. Mitchell, G. Pellerin, M. Buehner, M. Charron, L. Spacek, and B. Hansen, 2005: Atmospheric data assimilation with an ensemble Kalman filter: Results with real observations. *Mon. Wea. Rev.*, **133**:604–620.

Karbou, F., E. Gérard, and F. Rabier, 2010: Global 4DVAR assimilation and forecast experiments using AMSU observations over land. Part I: Impacts of various land surface emissivity parameterizations. *Wea. Forecasting*, **25**:5–19.

Kleist, D. T., D. F. Parrish, J. C. Derber, R. Treadon, W-S. Wu, S. Lord, 2009: Introduction of the GSI into the NCEP Global Data Assimilation System. *Wea. Forecasting*, **24**:1691-1705.

Liu, H., J. Anderson, Y-H. Kuo, and K. Raeder, 2007: Importance of forecast error multivariate correlations in idealized assimilation of GPS radio occultation data with the ensemble adjustment filter. *Mon. Wea. Rev.*, **135**:173–185.

Meng, Z. and F. Zhang, 2008: Tests of an ensemble Kalman filter for mesoscale and regional-scale data assimilation. Part II: Comparison with 3DVAR in a real-data case study. *Mon. Wea. Rev.*, **136**:522–540.

Parrish, D. F. and J. Derber, 1992: The National Meteorological Center's spectral and statistical-interpolation analysis system. *Mon. Wea. Rev*, **120**:1747–1763.

Petty, G. W., 2004. A First Course in Atmospheric Radiation. Sundog Publishing, Madison Wisconsin, 442 pp.

Rawlins, F., S. P. Ballard, K. J. Bovis, A. M. Clayton, D. Li, G. W. Inverarity, A. C. Lorenc, and T. J. Payne, 2007: The Met Office global 4-Dimensional data assimilation system. *Quart. J. Roy. Meteor. Soc.*, **133**:347–362.

Skamarock, W. C., J. B. Klemp, J. Dudhia, D. O. Gill, D. M. Barker, M. G. Duda, X-Y Huang, W. Wang, and J. G. Powers, 2008: A description of the Advanced Research WRF version 3. NCAR Tech Note NCAR/TN-475+STR, 113 pp. [Available from UCAR Communications, P. O. Box 3000, Boulder, CO 80307.]

Whitaker, J. S., T. M. Hamill, X. Wei, Y. Song, and Z. Toth, 2008: Ensemble data assimilation with the NCEP Global Forecast System. *Mon. Wea. Rev.*, **136**:463–482.

Xu, J, S. Rugg, L. Byerle, and Z. Liu, 2009a. Weather Forecasts by the WRF-ARW Model with the GSI Data Assimilation System in the Complex Terrain Areas of Southwest Asia. *Wea. Forecasting*, **24**: 987-1008.

Xu, J., S. Rugg, M. Horner, and L. Byerle, 2009b: Application of ATOVS radiance with ARW WRF/GSI data assimilation system in the prediction of Hurricane Katrina. *Open Atmos. Sci. J.*, **3**:13–28.

Zapotocny, T. H., W. P. Menzel, J. A. Jung, and J. P. Nelson III, 2005: A four-season impact study of rawinsonde, GOES, and POES data in the Eta Data Assimilation System. Part II: Contribution of the components. *Wea. Forecasting*, **20**:178–198.

Zapotocny, T. H., J. A. Jung, J. F. Le Marshall, and R. E. Treadon, 2007: A two-season impact study of satellite and in situ data in the NCEP Global Data Assimilation System. *Wea. Forecasting*, **22**:887–909.